TITLE: Development of low-cost biomass-based adsorbents for postcombustion CO_2 capture

AUTHORS: M.G. Plaza, C. Pevida, B. Arias, J. Fermoso, M.D. Casal, C.F. Martín, F. Rubiera, J.J. Pis

ADDRESS: Instituto Nacional del Carbón, CSIC. Apartado 73. 33080 Oviedo, Spain

***Corresponding author:** C. Pevida

Instituto Nacional del Carbón, C.S.I.C.

Apartado 73

33080 Oviedo (Spain)

Tel.: +34 985 11 90 90

Fax: +34 985 29 76 62

E-mail address: cpevida@incar.csic.es

Development of low-cost biomass-based adsorbents for postcombustion CO_2 capture

M.G. Plaza, C. Pevida, B. Arias, J. Fermoso, M.D. Casal, C.F. Martín, F. Rubiera, J.J. Pis

Instituto Nacional del Carbón, CSIC. Apartado 73. 33080 Oviedo, Spain

Abstract

In this work a series of carbon adsorbents were prepared from a low-cost biomass residue, olive stones. Two different approaches were studied: activation with CO_2 and heat treatment with gaseous ammonia. The results showed that both methods are suitable for the production of adsorbents with a high CO_2 adsorption capacity, and their potential application in VSA or TSA systems for postcombustion CO_2 capture. It was found that the presence of nitrogen functionalities enhances CO_2 adsorption capacity, especially at low partial pressures.

Keywords: CO_2 capture, adsorption, activated carbon, amination, activation

1. Introduction

Currently the energy system is mostly based on fossil fuels combustion; coal being the dominant fuel, power generation is responsible for about 1/3 of all anthropogenic CO_2 emissions. Moreover, related emissions are increasing rapidly due to the current growth in global energy demand. At the same time, there is an urgent need to stabilise the concentration of CO_2 in the atmosphere before permanent and severe damage to the climate system is done [1]. Although important measures are being taken, such as increasing the share of renewables, or improving the efficiency of energy conversion processes, it is widely accepted that Carbon Dioxide Capture and Storage, commonly referred as CCS, will be necessary if the demand for energy is to be satisfied, without contributing to global warming in the forthcoming years, while alternatives to fossil fuels are developed.

The capture or separation step is the main contributor to the overall cost of CCS [2]. At present, the preferred technology to carry out the separation of CO_2 in postcombustion applications is amine scrubbing. However, this technology presents a series of drawbacks,

such as the high energy requirement for the regeneration of the solvent. Other technologies in a lesser stage of development that seek to reduce the cost associated to the capture step include adsorption with activated carbons or zeolites. Recently it was reported that the cost associated to CO_2 capture can be reduced below the amine base case by using the technology of adsorption [3, 4].

Activated carbons present a series of advantages as CO_2 adsorbents: a high adsorption capacity at ambient pressures, ease of regeneration, low cost, and insensitiveness to moisture. These materials can be obtained from almost any carbonaceous product by carbonisation followed by an activation step. The adsorption capacity of an activated carbon is mainly governed by its texture but it is also strongly influenced by the surface chemistry. The presence of nitrogen functionalities in the carbon surface have been reported to be effective in the adsorption of acid gases, such as H_2S and SO_2 [5, 6]. Attention has also been given to the introduction of nitrogen functionalities into the carbon in order to enhance CO_2 adsorption capacity [7-13]. Other possibilities include the introduction of nitrogen into the carbon matrix by reaction with gaseous ammonia at high temperatures [14-20].

In this study two different approaches for developing efficient carbon dioxide adsorbents were compared: activation with carbon dioxide, and heat treatment with gaseous ammonia, which will be referred to from now on as amination. The main objective of amination is the introduction of basic nitrogen functionalities to enhance CO_2 adsorption.

2. Experimental

A biomass by-product from the Spanish food industry, olive stones (OS), was selected as starting material for the preparation of the activated carbons. The olive stones were ground and sieved, and a particle size between 1 and 3 mm was selected. First, carbonisation was carried out at 600 ºC under an inert atmosphere of N_2. An average char yield of 24 % was obtained. The resulting char was denoted as GKOS.

A first series of samples were prepared by activation of the char with 10 cm^3 min^{-1} of carbon dioxide at different burn-off degrees (20, 40 and 50 %). The temperature of activation was set at 800 ºC, based on previous tests in a thermogravimetric analyser. The activated samples were referred to as GKOSAX, where A represents activation, and X the degree of the burn-off.

A second series of samples were obtained by heat treating the char with 50 cm^3 min^{-1} of ammonia gas at four different temperatures: 400, 600, 800 and 900 ºC. The soaking time was 2 h in all cases. These samples were denoted as GKOSNY, where N stands for NH_3, and Y represents the temperature of the treatment.

Chemical characterisation of the samples involved the determination of the proximate and ultimate analyses, and the estimation of the point of zero charge (pH_{PZC}) by a mass titration method adapted from Noh and Schwarz [21].

All the samples were characterised by physical adsorption of N_2 and CO_2 at -196 ºC and 0 ºC, respectively, in a volumetric apparatus (Micromeritics Tristar 3000). Prior to the adsorption measurements, the samples were outgassed overnight at 100 ºC under vacuum. The use of both adsorbates provides complementary information about the porous texture of the samples: the adsorption of CO_2 at 0 ºC and up to 1 bar is restricted to pores narrower than 1 nm, whereas N_2 adsorption at -196 ºC covers wider pore sizes but presents diffusion limitations in the narrowest pores. The apparent surface area of the samples was evaluated from the N_2 adsorption isotherms by applying the BET equation in the linear form proposed by Parra *et al* [22]. The mesopore volume (V_{meso}) was assessed from the N_2 adsorption isotherm by the Density Functional Theory (DFT), assuming slit shape pores geometry and non regularisation [23]. The narrow micropore volume (W_0) (pore width below 0.7 nm) was estimated from the CO_2 adsorption isotherms at 0 ºC by the Dubinin-Radushkevich method [24].

The CO_2 capture capacity of the adsorbents was evaluated in a Setaram TGA 92 thermogravimetric analyser. CO_2 uptakes were determined from the mass evolution profiles when the samples were exposed to a gas flow containing CO_2. Prior to the adsorption measurements, the samples were dried at 100 ºC in 50 cm^3 min^{-1} of Ar for 1h.

3. Results and discussion

As can be seen from the chemical analysis presented in Table 1, the raw biomass shows high volatile matter and low ash and sulphur contents. After carbonisation, the char exhibits a carbon content above 90 % and a low ash content, being a suitable precursor for activated carbon production. The oxygen content is substantially reduced during the carbonisation step as it is associated to the volatile matter of the biomass. However, the char still shows a noticeable oxygen content that may play an important role not only in adsorption processes but also in surface reactions with ammonia.

The point of zero charge experiences an increase after carbonisation, mainly as a consequence of the loss of surface functionalities. The char has a pH_{PZC} of 8.7, which indicates the dominant basic character of its surface. This basicity may result from basic surface oxides formed after carbonisation [25], or from non-heteroatomic Lewis base sites, that are characterised by regions of π electron density on the carbon basal planes [26].

Figure 1 shows the DRIFT spectra of the raw olive stones, OS, and of the carbonised product, GKOS. In the spectrum of the raw biomass, it can be observed the presence of IR bands associated to aliphatic carbon (near 2900 cm^{-1}), phenolic groups (3000-3600 and 1000-1200 cm^{-1}) and also a band at 1740 cm^{-1} compatible with the presence of carboxyl or lactone groups [27, 28]. The bands at 2900 and 1740 cm^{-1} have disappeared completely as a consequence of the carbonisation treatment, indicating an increase in the aromaticity of the carbon and the loss of labile carboxylic acids. The spectrum of the char also shows an intensification of the band at 1600 cm^{-1} that can be associated to quinone groups [27, 28]. This band, together with

the overlapping bands between 1000 and 1500 cm^{-1} have also been attributed to carboxyl-carbonate structures [29, 30]. The presence of these basic oxides helps to explain the basicity of the char and its relatively high oxygen content.

3.1. Activation

3.1.1. Characterisation of the activated samples

Activation with carbon dioxide is an oxidative treatment that eliminates C atoms from the char by means of a heterogeneous reaction that releases gaseous CO. During the gasification reaction, some oxygen may be chemisorbed on the carbon surface, forming C(O) surface complexes [31]. To study the type of oxygen functionalities present in the samples, temperature programmed desorption tests (TPD) were carried out in a thermogravimetric analyser coupled to an Omnistar MS spectrometer. It is well known that upon heating in an inert atmosphere, the oxygen surface complexes of carbonaceous materials decompose, releasing CO_2 and CO [32]. CO_2 results from the decomposition of carboxyls, lactones and anhydrides, while CO comes from anhydrides, phenols, carbonyls, quinones and pyrones [20, 32, 33].

Figure 2 shows the profiles of evolved CO_2 and CO for samples GKOS and GKOSA50, in the course of heating at 15 ºC min^{-1} in 50 cm^3 min^{-1} of Ar. The char presents two maxima in the CO_2 profile: at around 350 and 700 ºC. Low temperature CO_2 is commonly attributed to the decomposition of carboxyls, while higher temperature CO_2 is associated to the decomposition of lactones or anhydrides [27]. However, as previously discussed, the DRIFT spectrum of GKOS does not show any characteristic band at 1750 cm^{-1}, typical of those species. The presence of carboxyl-carbonates was also reported [29, 30]. These groups could release CO_2 upon heating, which would explain the CO_2 emissions from GKOS. GKOSA50 presents similar CO_2 evolution regions to GKOS, but it also shows CO_2 contributions at lower temperatures. This low temperature CO_2 may result from the decomposition of labile

carboxyls formed by oxygen chemisorption after the activation process [34]. Similarly to GKOS, the narrow peak at 670 ºC cannot come from the decomposition of anhydrides, as there is no simultaneous evolution of CO. However, the largest change in oxygen functionalities after activation can be observed from the CO profile. The CO profile of GKOS presents a maximum at 770 ºC, which can be attributed to the decomposition of phenols, there being a shoulder at 630 ºC which may be related to quinones [35], in good agreement with the DRIFT spectrum. On the other hand, GKOSA50 shows a single peak centred at 950 ºC that matches a smaller shoulder in the CO profile of GKOS. This high temperature CO has been attributed to pyrone groups [35].

As can be seen in Table 2, activated samples have higher values of pH_{PZC} than the corresponding char. This increase in surface basicity may partly be a consequence of the extended heat treatment at a temperature higher than that of the carbonisation step. However, it may also be due to the formation of basic pyrone-type functionalities during the activation process [36]. The presence of these basic oxygen functionalities can have an enhancing effect on the adsorption of acidic CO_2, as has been demonstrated for SO_2 [36, 37].

The N_2 adsorption isotherms of the activated olive stones are shown in Figure 3a. All the activated samples presented type I nitrogen adsorption isotherms, characteristic of microporous materials. From the amount of adsorbed nitrogen it can be seen that activation with carbon dioxide substantially develops the texture of the starting char. The textural parameters calculated from the N_2 adsorption isotherms of the activated samples are summarised in Table 2. It can be seen that the char presents higher narrow micropore volume (W_0) than total pore volume in nitrogen (V_p). This is due to diffusion restrictions on the adsorption of N_2 at -196 ºC on narrow micropores [38]. As activation proceeds, the microporosity widens, allowing the N_2 to enter the pores as reflected by the increase in V_p. Activation with CO_2 produces leads to the continuous development of the char porous

structure resulting in BET apparent surface areas of up to 1079 m^2 g^{-1} and total pore volumes of up to 0.5 cm^3 g^{-1}. The predominantly microporous character of the samples is reflected by the small contribution of the mesopore volume to the total pore volume, even for high degrees of burn-off.

Figure 3b shows the CO_2 adsorption isotherms of the activated olive stones. It can be observed that the shape of the isotherms tends to be more rectilinear as the burn-off increases. This is due to the gradual widening of the micropores with activation. For low burn-off degrees, the formation of narrow microporosity prevails (see the increase in W_0 in Table 2). However, as the activation process proceeds, the narrow micropores widen, resulting in wider microporosity (pore widths below 2 nm) and mesoporosity (pore widths between 2 and 50 nm). Thus, from the point of view sample texture, activation results in the continuous increase of V_p with burn-off degree, while W_0 goes through a maximum for GKOSA40, decreasing at higher burn-off degrees.

3.1.1.1. CO_2 capture tests

Table 3 summarises the CO_2 capture capacities of the activated samples at 25 ºC and 100 ºC, obtained in 50 cm^3 min^{-1} of CO_2. The CO_2 uptakes are expressed in terms of mass of CO_2 per mass of dry adsorbent. As might be expected for a physisorption process the adsorption capacity of the carbons decreases with increasing adsorption temperature. All the activated samples present higher CO_2 capture capacities than that of the initial char at both temperatures, due to the substantial textural development during activation. Moreover, at 25 ºC, CO_2 capture capacity reaches values of up to 10.7 wt.%, which is greater than that of commercial activated carbons tested under the same experimental conditions [7]. Even at 100 ºC, the samples still present significant capacities of up to 3.2 wt.%. This is a very interesting advantage, as the cooling of flue gas that is required prior to the adsorption unit can be reduced if the capture step can be carried out at higher temperatures. The possibility of using

lower adsorption temperatures would increase the working capacity of the adsorbents making it possible to reduce the size of the adsorption equipment. However cooling costs would then increase. Therefore, these parameters would need to be balanced in order to optimise the cost of the capture step.

Production yields of the produced olive stone activated carbons exceed in all cases 12 %, which is above the yield of commercial wood-based carbons [39]. However, an increase in the burn-off degree would be justified, economically speaking, if a significant increase in the working capacity of the adsorbent was attained. Thus, in the case of olive stones, increasing the burn-off above 40 % could not be justified by an increase in CO_2 adsorption capacity.

3.2. Amination

3.2.1. Characterisation of the aminated samples

Table 4 summarises the chemical and textural characterisation results of the aminated samples. Amination significantly increases the amount of nitrogen incorporated into the carbon matrix. This nitrogen fixation comes from the reaction of ammonia with carbon surface oxides to form ammonium salts and amine groups that, upon dehydration and dehydrogenation produce amides, nitriles and pyridine or pyrrole-like functionalities [16, 40]. The nitrogen content obtained is relatively high, considering that the chars were not subjected to oxidation prior to the ammonia treatment, as is customary in the literature [19]. Nitrogen fixation seems to be favoured at high temperatures, as the maximum nitrogen content was obtained for the sample aminated at 800 ºC. The pH_{PZC} of the samples also increases after amination, parallel to the incorporation of nitrogen, reflecting the basic nature of the functionalities formed. Previous studies carried out by our group have shown that the type of nitrogen functionality incorporated may vary with the temperature of ammonia treatment: in the case of the samples obtained above 600 ºC, nitrogen is incorporated onto the layer system of the carbon as thermally stable pyrrol and pyridinic-type functionalities, while in the case of

the samples obtained at lower temperatures, nitrogen might be forming amide-like functionalities [7].

Figure 4a shows the N_2 adsorption isotherms of the aminated olive stones. It can be seen from the isotherms that amination has caused the porous structure of the char to develop by partial gasification. Ammonia is known to decompose at high temperatures producing atomic H and NH_2 and NH radicals that react with the carbon releasing gaseous H_2, CH_4, HCN and $(CN)_2$ [14, 18]. The gasification becomes more important as the temperature increases, producing a continuous increase in the BET surface area and in the total pore volume. From the CO_2 isotherms in Figure 4b, it can be seen that the formation of new microporosity is important at 800 ºC. Below this temperature, the CO_2 isotherms of the initial char and the aminated samples at 400 and 600 ºC are almost coincident. By comparing the narrow micropore volume (W_0), obtained from the CO_2 adsorption isotherms, with the total pore volume (V_p), obtained from the N_2 adsorption isotherms, presented in Table 4, it can be observed that the total pore volume is smaller in all the samples. As it has been previously discussed, this is due to diffusion limitations impeding the entry of the N_2 molecule at -196 ºC into the narrow micropores. Thus, the new microporosity formed by gasification with ammonia is of very narrow size.

The total production yields of the aminated samples are presented in Table 5 (g of final adsorbent per 100 g of raw biomass). Only the samples aminated at high temperatures present lower yields than the char, due to the contribution of gasification. Even so, the yields are still above those of the activated samples (cf. Table 3).

3.2.2. CO_2 capture test of the aminated samples

Table 5 summarises the CO_2 capture capacity of the aminated samples in 50 $cm^3\ min^{-1}$ of CO_2 flow at 25 and 100 ºC. Again a decrease in adsorption capacity with increasing temperature can be observed. The maximum capacities were obtained at both temperatures for the sample

aminated at 800 ºC. This sample is also the one with the highest nitrogen content, which is thought to be the main cause of its high CO_2 uptake. Moreover, the adsorption capacity of GKOSN800 is very similar to that of the sample activated to 20 % burn-off, GKOSA20, although the latter experienced significantly higher textural development as a result of which higher CO_2 adsorption capacities might have been expected. Thus, the introduction of nitrogen functionalities seems to be playing an important role in CO_2 adsorption.

Adsorption is favoured at low temperature and high adsorbate partial pressures. Hence, the working capacity of the adsorbents in a real postcombustion application, where CO_2 is diluted in a flue gas containing mainly nitrogen, will be lower than that achieved in pure CO_2. In order to study the behaviour of the adsorbents in more realistic postcombustion conditions, adsorption tests in a gas mixture containing 15 % CO_2 and 85 % N_2 at 40 ºC and 1 bar were carried out in a thermobalance for selected samples. This temperature was chosen as being feasible if the capture unit is to be placed after the desulphuration step in the power plant.

Samples were completely regenerated by changing the feed gas to Ar and increasing the temperature to 100 ºC. The corresponding mass profiles are presented in Figure 5. In these conditions, the capture capacity of the adsorbents is reduced to below 3 wt.%. However, it is important to note that the sequence of increasing CO_2 capture capacity has been altered. In pure CO_2 the adsorption capacity of the samples followed the order: GKOSA50 ≈ GKOSA40 > GKOSN800 while for a CO_2 concentration of 15 % the relative order was: GKOSA40 > GKOSN800 > GKOSA50. This would seem to indicate that the effect of the surface area of the carbon becomes less important as the partial pressure of CO_2 decreases. On the other hand, other factors, such as the presence of nitrogen functionalities or a narrower pore size distribution, seem to play a more important role. GKOSA40 presents a lower total pore volume and surface area than GKOSA50, but narrower pore sizes that appear to be more efficient for adsorbing CO_2.

Conclusions

Basic activated carbons with a CO_2 capture capacity of up to 10.7 wt.% at 25 ºC and up to 3.2 wt.% at 100 ºC in pure CO_2 were produced from olive stones, a low cost biomass by-product, by means of activation with carbon dioxide. These capacities exceed those of commercial activated carbons. The basic surface oxides formed during the carbonisation and activation processes may have a beneficial effect on the adsorption of CO_2. The pore size distribution has been shown to play an important role in CO_2 adsorption, especially at low partial pressures.

Heat treatment with gaseous ammonia is proposed as an alternative pathway to produce efficient CO_2 adsorbents. Nitrogen was successfully incorporated into the carbon structure without the need for a previous oxidation step, and it has been demonstrated to have an enhancing effect on CO_2 adsorption. The effect of the temperature of the treatment was also studied. 800 ºC was found to be the optimum temperature as CO_2 adsorption capacity and nitrogen incorporation reach the maximum values. CO_2 capture capacities of up to 8.6 wt.% at 25 ºC and 2.6 wt.% at 100 ºC in pure CO_2 were obtained for the aminated samples. These values are similar to, or even substantially greater at temperatures above ambient, than those of commercial activated carbons. Amination has other advantages over activation including shorter soaking times and higher production yields per gram of initial biomass. What is more, adsorption tests in a gas mixture containing 15 % of CO_2 revealed that the effect of surface nitrogen is more noticeable at lower partial pressures of CO_2.

Acknowledgements

This work was carried out with financial support from the Spanish MEC (Project CTM2005-03075/TECNO). M.G.P., C.F.M. and J.F. acknowledge funding from the CSIC I3P Program co-financed by the European Social Fund, CSIC JAE Program and Plan Regional de Investigación del Principado de Asturias, respectively.

References

[1] IPCC, *Climate change 2007: the physical science basis*. 2007, IPCC: Cambridge, United Kingdom and New York, NY, USA. p. 996.

[2] IPCC, *IPCC special report on carbon dioxide capture and storage*. 2005, IPCC: Cambridge, United Kingdom and New York, NY, USA. p. 442.

[3] Radosz M, Hu X, Krutkramelis K, Shen Y. Flue-Gas Carbon Capture on Carbonaceous Sorbents: Toward a Low-Cost Multifunctional Carbon Filter for "Green" Energy Producers. Ind Eng Chem Res 2008;47:3783-94.

[4] Ho MT, Allinson GW, Wiley DE. Reducing the Cost of CO_2 Capture from Flue Gases Using Pressure Swing Adsorption. Ind Eng Chem Res 2008;47:4883-90.

[5] Adib F, Bagreev A, Bandosz TJ. Adsorption/Oxidation of Hydrogen Sulfide on Nitrogen-Containing Activated Carbons. Langmuir 2000;16:1980-6.

[6] Bagreev A, Bashkova S, Bandosz TJ. Adsorption of SO_2 on Activated Carbons: The Effect of Nitrogen Functionality and Pore Sizes. Langmuir 2002;18:1257-64.

[7] Pevida C, Plaza MG, Arias B, Fermoso J, Rubiera F, Pis JJ. Surface modification of activated carbons for CO_2 capture. Appl Surf Sci 2008;254:7165-72.

[8] Plaza MG, Pevida C, Arias B, Fermoso J, Arenillas A, Rubiera F, Pis JJ. Application of thermogravimetric analysis to the evaluation of aminated solid sorbents for CO_2 capture. J Therm Anal Calorim 2008;92:601-6.

[9] Plaza MG, Pevida C, Arenillas A, Rubiera F, Pis JJ. CO_2 capture by adsorption with nitrogen enriched carbons. Fuel 2007;86:2204-12.

[10] Drage TC, Arenillas A, Smith KM, Pevida C, Piippo S, Snape CE. Preparation of carbon dioxide adsorbents from the chemical activation of urea-formaldehyde and melamine-formaldehyde resins. Fuel 2007;86:22-31.

[11] Maroto-Valer MM, Lu Z, Zhang Y, Tang Z. Sorbents for CO_2 capture from high carbon fly ashes. Waste Manage 2008; In Press

[12] Maroto-Valer MM, Tang Z, Zhang Y. CO_2 capture by activated and impregnated anthracites. Fuel Process Technol 2005;86:1487-502.

[13] Przepiórski J, Skrodzewicz M, Morawski AW. High temperature ammonia treatment of activated carbon for enhancement of CO_2 adsorption. Appl Surf Sci 2004;225:235-42.

[14] Boehm HP, Mair G, Stoehr T, De Rincon AR, Tereczki B. Carbon as a catalyst in oxidation reactions and hydrogen halide elimination reactions. Fuel 1984;63:1061-3.

[15] Meldrum BJ, Rochester CH. In situ infrared study of the surface oxidation of activated carbon in oxygen and carbon dioxide. J Chem Soc, Faraday Trans 1990;86:861-5.

[16] Stohr B, Boehm HP, Schlogl R. Enhancement of the catalytic activity of activated carbons in oxidation reactions by thermal treatment with ammonia or hydrogen cyanide and observation of a superoxide species as a possible intermediate. Carbon 1991;29:707-20.

[17] Biniak S, Szymanski G, Siedlewski J, Swiatkowski A. The characterization of activated carbons with oxygen and nitrogen surface groups. Carbon 1997;35:1799-810.

[18] Bota KB, Abotsi GMK. Ammonia: a reactive medium for catalysed coal gasification. Fuel 1994;73:1354-7.

[19] Jansen RJJ, van Bekkum H. Amination and ammoxidation of activated carbons. Carbon 1994;32:1507-16.

[20] Vinke P, van der Eijk M, Verbree M, Voskamp AF, van Bekkum H. Modification of the surfaces of a gas activated carbon and a chemically activated carbon with nitric acid, hypochlorite, and ammonia. Carbon 1994;32:675-86.

[21] Noh JS, Schwarz JA. Estimation of the point of zero charge of simple oxides by mass titration. J Colloid Interface Sci 1989;130:157-64.

[22] Parra JB, de Sousa JC, Bansal RC, Pis JJ, Pajares JA. Characterization of activated carbons by the BET equation - an alternative approach. Adsorpt Sci Technol 1995;12:51-65.

[23] Olivier JP. Improving the models used for calculating the size distribution of micropore volume of activated carbons from adsorption data. Carbon 1998;36:1469-72.

[24] Dubinin MM. Properties of active carbons. In: Walker JPL, editors. Chemistry and physics of carbon, New York: Marcel Dekker Inc; 1966, p. 51-120.

[25] Papirer E, Li S, Donnet J-B. Contribution to the study of basic surface groups on carbons. Carbon 1987;25:243-7.

[26] Bandosz TJ, Ania CO. Surface chemistry of activated carbons and its characterization. In: Bandosz TJ, editors. Activated carbon surfaces in environmental remediation, Amsterdam: Elsevier Ltd.; 2006.

[27] Figueiredo JL, Pereira MFR, Freitas MMA, Órfão JJM. Modification of the surface chemistry of activated carbons. Carbon 1999;37:1379-89.

[28] Fanning PE, Vannice MA. A DRIFT study of the formation of surface groups on carbon by oxidation. Carbon 1993;31:721-30.

[29] Zawadzki J. IR spectroscopy studies of oxygen surface compounds on carbon. Carbon 1978;16:491-7.

[30] Ishizaki C, Martí I. Surface oxide structures on a commercial activated carbon. Carbon 1981;19:409-12.

[31] Fritz OW, Hüttinger KJ. Active sites and intrinsic rates of carbon-gas reactions--a definite confirmation with the carbon-carbon dioxide reaction. Carbon 1993;31:923-30.

[32] Tremblay G, Vastola FJ, Walker PL. Thermal desorption analysis of oxygen surface complexes on carbon. Carbon 1978;16:35-9.

[33] Otake Y, Jenkins RG. Characterization of oxygen-containing surface complexes created on a microporous carbon by air and nitric acid treatment. Carbon 1993;31:109-21.

[34] Rodríguez-Reinoso F, Pastor AC, Marsh H, Huidobro A. Preparation of activated carbon cloths from viscous rayon: Part III. Effect of carbonization on CO_2 activation. Carbon 2000;38:397-406.

[35] Haydar S, Moreno-Castilla C, Ferro-García MA, Carrasco-Marín F, Rivera-Utrilla J, Perrard A, Joly J-P. Regularities in the temperature-programmed desorption spectra of CO_2 and CO from activated carbons. Carbon 2000;38:1297-308.

[36] Carrasco-Marin F, Utrera-Hidalgo E, Rivera-Utrilla J, Moreno-Castilla C. Adsorption of SO_2 in flowing air onto activated carbons from olive stones. Fuel 1992;71:575-8.

[37] Davini P. Adsorption of sulphur dioxide on thermally treated active carbon. Fuel 1989;68:145-8.

[38] Rodríguez-Reinoso F, Linares-Solano A, Martín-Martínez JM, López-González JD. The controlled reaction of active carbons with air at 350°C–II: Evolution of microporosity. Carbon, 1984;22:123-30.

[39] Menendez-Díaz JA, Martín-Gullón I. Types of carbon adsorbents and their production. In: Bandosz TJ, editors. Activated carbon surfaces in environmental remediation, New Yok: Elsevier Ltd; 2006.

[40] Jansen RJJ, van Bekkum H. XPS of nitrogen-containing functional groups on activated carbon. Carbon 1995;33:1021-7.

List of tables

Tables

Table 1 Chemical analysis of the raw biomass (OS) and the resulting char (GKOS)

Sample	pH_{PZC}	Proximate analysis (%, db)			Ultimate analysis (%, daf)				
		VM	Ash	FC*	C	H	N	S	O
OS	6.2	85.4	0.8	13.8	51.6	6.0	0.2	0.5	41.7
GKOS	8.7	9.8	1.6	88.6	93.0	2.2	0.3	0.0	4.5

VM: volatile matter; FC: fixed carbon; * calculated by difference; db: dry basis; daf: dry ash free basis

Table 2 Point of zero charge and textural characterisation of the activated samples

Sample	pH_{PZC}	N_2 adsorption at -196 ºC			CO_2 adsorption at 0 ºC
		S_{BET} ($m^2\ g^{-1}$)	V_p [a] ($cm^3\ g^{-1}$)	V_{meso} [b] ($cm^3\ g^{-1}$)	W_0 ($cm^3\ g^{-1}$)
GKOS	8.7	43	0.026	-	0.173
GKOSA20	9.8	613	0.288	0.046	0.294
GKOSA40	9.5	909	0.437	0.073	0.296
GKOSA50	9.6	1079	0.502	0.066	0.246

[a] Total pore volume estimated by the amount of adsorbed nitrogen (as liquid) at $p/p^0 = 0.99$

[b] Volume of mesopores (2 < pore width < 50 nm) obtained from the DFT method

Table 3 Product yield of the activated samples and CO_2 capture capacity at 25 and 100 ºC in pure CO_2 (50 cm^3 min^{-1})

Sample	Product yield (%)	CO_2 capture capacity (wt.%)	
		25 ºC	100ºC
GKOS	24	5.8	1.5
GKOSA20	19	8.9	2.9
GKOSA40	15	10.5	3.2
GKOSA50	12	10.7	3.2

Table 4 Chemical and textural characterisation of the aminated samples

Sample	N (%, db)	pH_{PZC}	N_2 adsorption at -196 ºC		CO_2 adsorption at 0 ºC
			S_{BET} (m^2g^{-1})	V_p ($cm^3\ g^{-1}$)	W_0 ($cm^3\ g^{-1}$)
GKOSN400	0.88	8.9	152	0.065	0.183
GKOSN600	2.58	9.2	232	0.100	0.174
GKOSN800	3.64	11.3	390	0.164	0.200
GKOSN900	3.06	10.9	442	0.189	0.209

Table 5 Product yield of the aminated samples and CO_2 capture capacity at 25 and 100 ºC in pure CO_2 (50 cm^3 min^{-1})

Sample	Product yield (%)	CO_2 capture capacity (wt.%)	
		25 ºC	100ºC
GKOS	24	5.8	1.5
GKOSN400	24	6.8	1.9
GKOSN600	23	7.1	2.1
GKOSN800	22	8.6	2.6
GKOSN900	19	7.3	2.5

List of figures

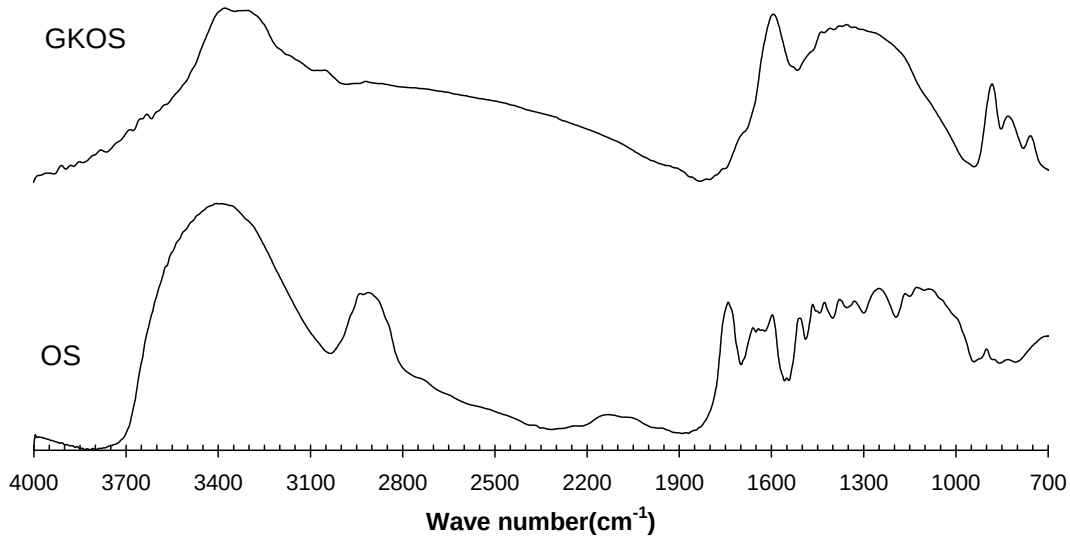

Figure 1. DRIFT spectra of the starting olive stones (OS) and the carbonised product (GKOS).

a)

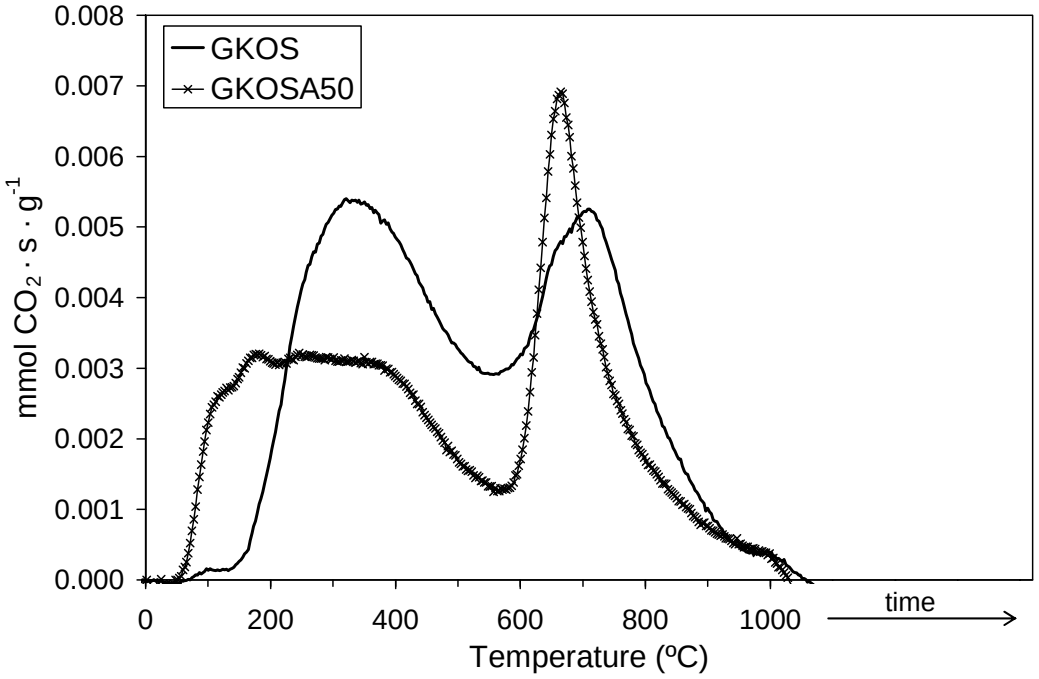

b)

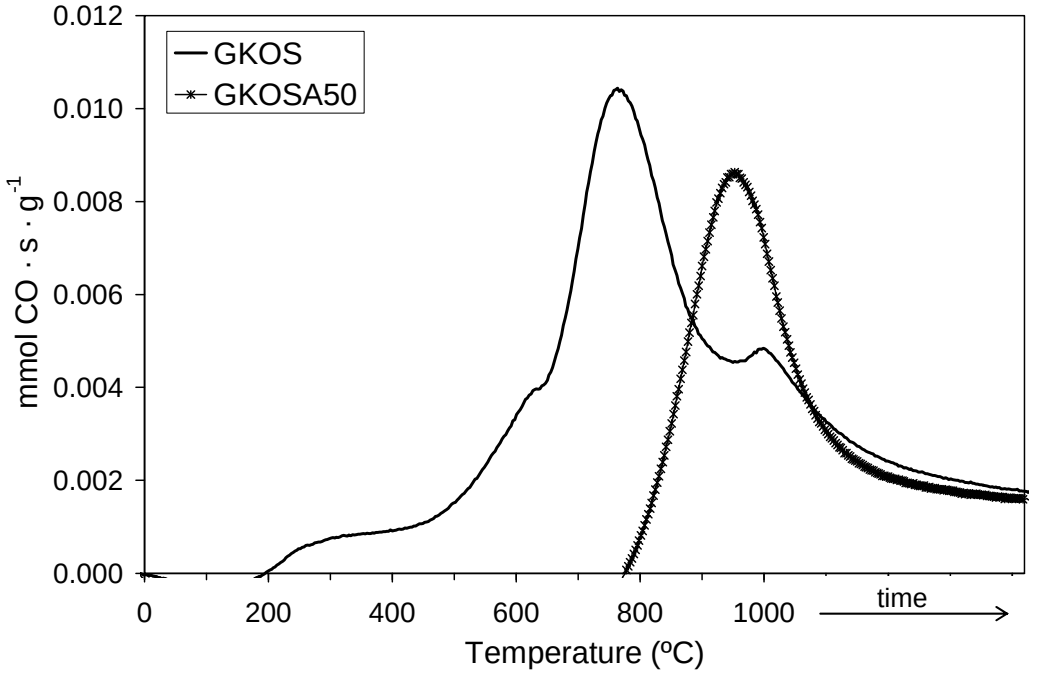

Figure 2. a) CO_2 and b) CO evolution profiles during temperature programmed desorption tests in 50 cm^3 min^{-1} of Ar (heating rate 15 ºC min^{-1} up to 1000 ºC).

a)

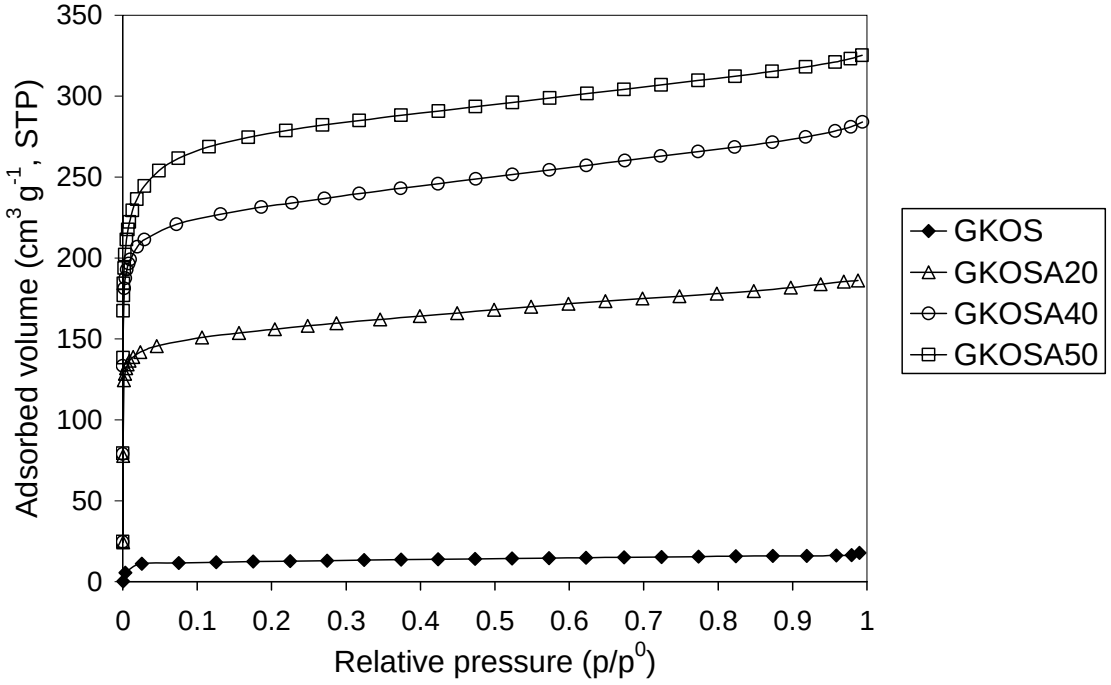

b)

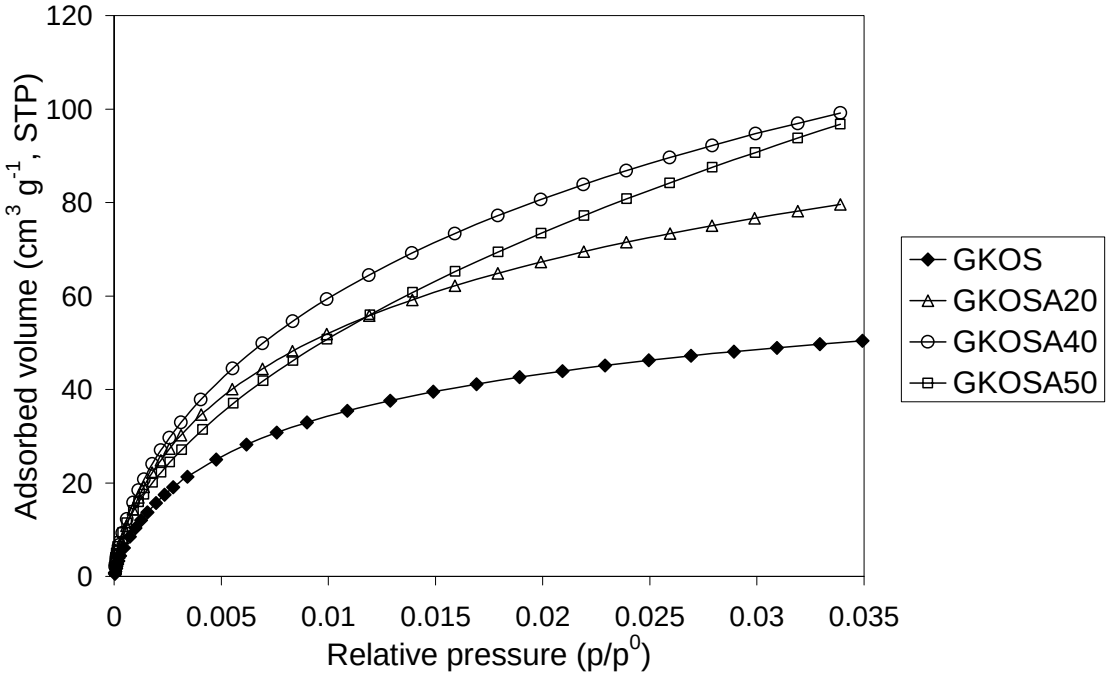

Figure 3. Adsorption isotherms of the activated olive stones: a) N_2 at -196 ºC and b) CO_2 at 0 ºC.

a)

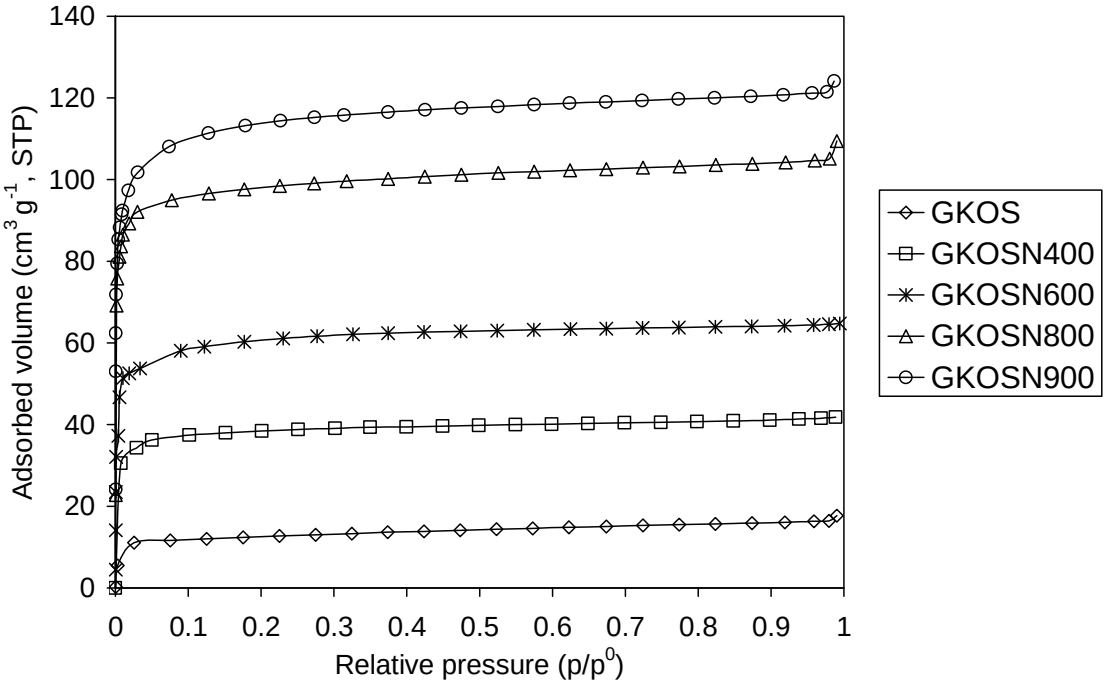

b)

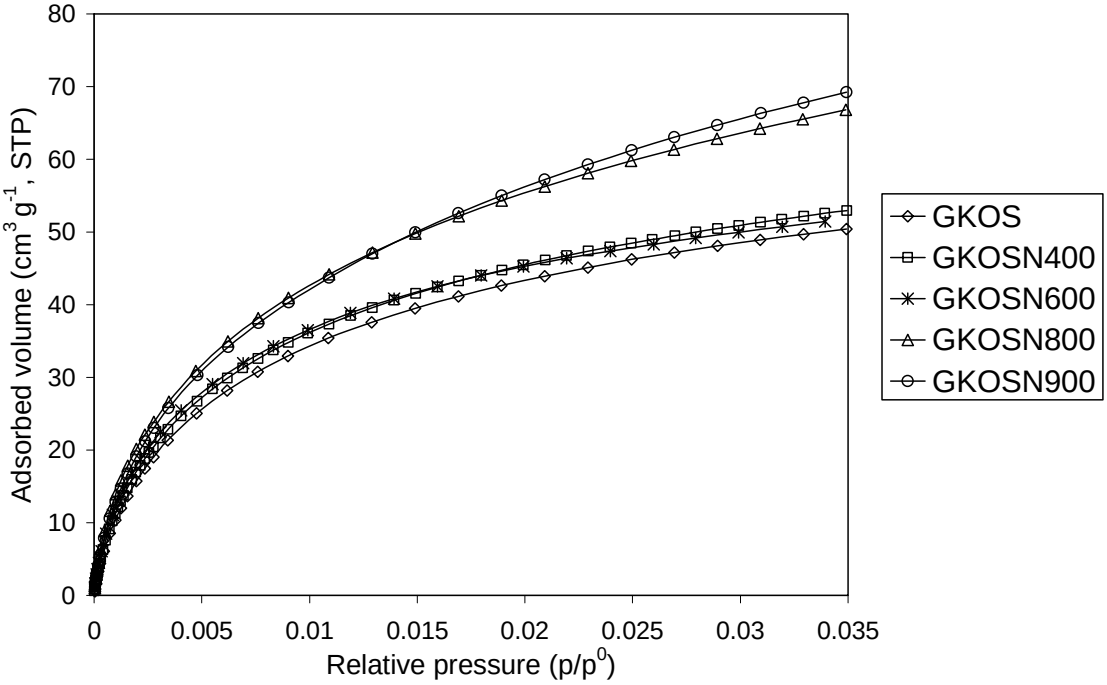

Figure 4. Adsorption isotherms of aminated olive stones: a) N_2 at -196 ºC and b) CO_2 at 0 ºC.

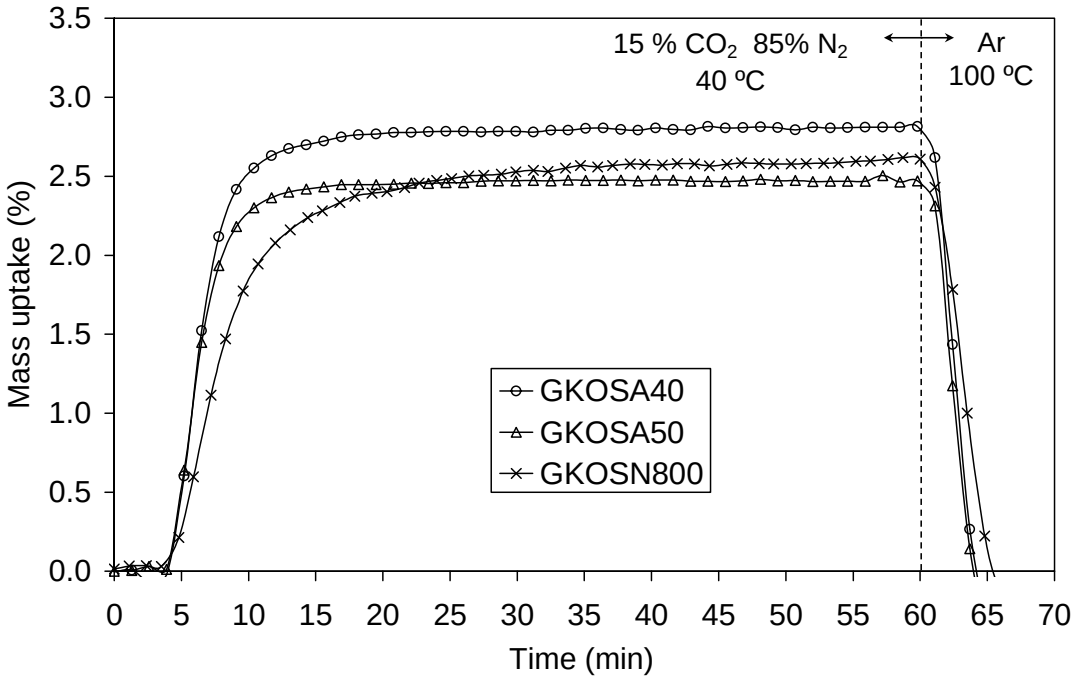

Figure 5. CO_2 capture tests in a gas mixture containing 15 % CO_2 and 85 % N_2.